Journal of Computer-Aided Molecular Design, 8 (1994) 29–40
ESCOM

J-CAMD 230

Coupling constants again: Experimental restraints in structure refinement

Dale F. Mierke[a], Thomas Huber[b] and Horst Kessler[b,*]

[a]*Department of Chemistry, Clark University, 950 Main Street, Worcester, MA 01610, U.S.A.*
[b]*Organisch Chemisches Institut, Technische Universität München, Lichtenbergstrasse 4, D-85747 Garching, Germany*

Received 14 September 1993
Accepted 1 October 1993

Key words: Structure refinement; Coupling constant restraints; Time-dependent restraints; Ensemble averages

SUMMARY

Utilization of coupling constants as restraints in computational structure refinement is reviewed. In addition, we address the effect of conformational averaging and examine different approaches to apply the restraints when the experimental observable is obviously a result of averaging. Here, two different computational methods are compared. The simulation of a single structure with time-dependent restraints produces results very similar to those obtained with the calculation of numerous copies of the molecule (an ensemble of structures) and ensemble averaging. The advantages and disadvantages of the two methods are illustrated with simulations of cyclosporin A, for which 117 NOEs and 62 homo- and heteronuclear coupling constants have been measured.

INTRODUCTION

Structure–activity relationships (SAR) are only as accurate as the structures on which they have been developed. The inherent flexibility of peptides is a hindrance to the development of SARs for peptidic drugs. Methods to overcome this problem include cyclization and the use of nonnatural amino acids which allow for the introduction of conformational constraints and specific conformational features (i.e., control the side-chain orientations) [1–9]. The development of more quantitative relationships requires structures of the highest quality. From the point of view of an experimentalist, this requires that as much experimental data as possible be utilized in the refinement of the conformation. In this regard, measurement of NOEs is the most important. However, for peptides, which we will concentrate on here, the number of NOEs is rather limited, when compared to proteins, because of a large ratio of surface area to core.

*To whom correspondence should be addressed.

Coupling constants are one source of conformational information which has been available for a long time in NMR investigations in solution. The conformational information is obtained from the equation developed by Karplus [10]:

$$^3J = A\cos^2(\theta) + B\cos(\theta) + C \quad (1)$$

which relates the coupling constant to the dihedral angle subtended by the coupled atoms, θ. For a long time coupling constants were used only as a secondary check of the structure, after the refinement procedure; a structure was developed from the NOEs and then the relevant dihedral angles compared to the answers obtained from Eq. 1. The problem arises from the multiple answers obtained from Eq. 1. A plot of Eq. 1 is shown in Fig. 1 (solid line) for ϕ and the homonuclear coupling constant $^3J_{HN\text{-}H\alpha}$, using A, B and C values of 9.4, −1.1 and 0.4, respectively [11]. In Fig. 1, an example coupling constant of 8 Hz, producing four possible ϕ dihedral angles, is indicated by a horizontal line.

One way of addressing the multiple answers from Eq. 1 is the measurement of more than one coupling constant about the given dihedral angle [11,12]. There are many additional coupling constants, especially heteronuclear coupling constants, that can be measured [11–24]; some examples for the backbone dihedral angle ϕ are given in Fig. 2. In addition to the homonuclear $^3J_{HN\text{-}H\alpha}$ there are two heteronuclear coupling constants, $^3J_{HN\text{-}C\beta}$ and $^3J_{CO\text{-}H\alpha}$, that can readily be measured, even in molecules with magnetically active heteronuclei in natural abundance. Each

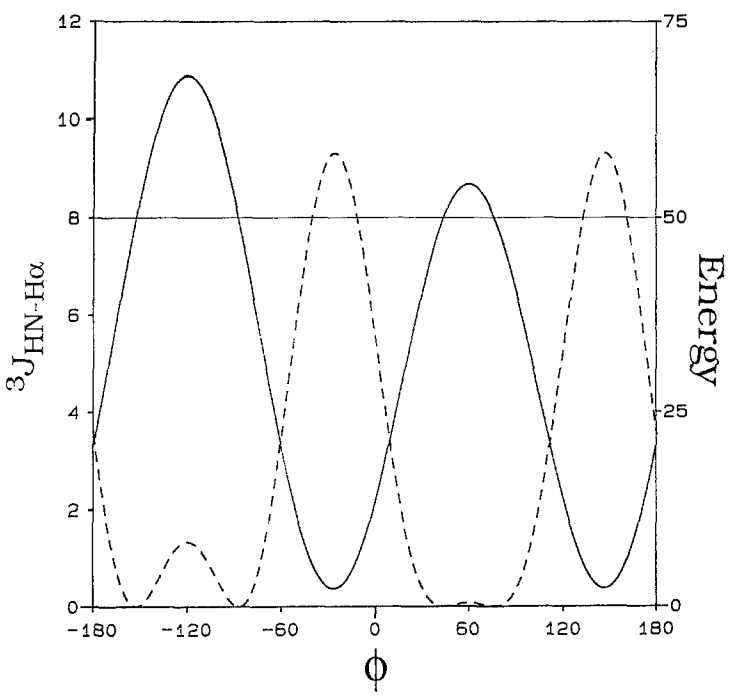

Fig. 1. An illustration of the Karplus curve, Eq. 1, using A, B and C coefficients of 9.4, −1.1 and 0.4, respectively (solid line). The four ϕ torsions from a $^3J_{HN\text{-}H\alpha}$ coupling constant of 8.0 Hz are shown with a horizontal line. The penalty function, Eq. 2, for a coupling of 8.0 Hz is shown as a dashed line.

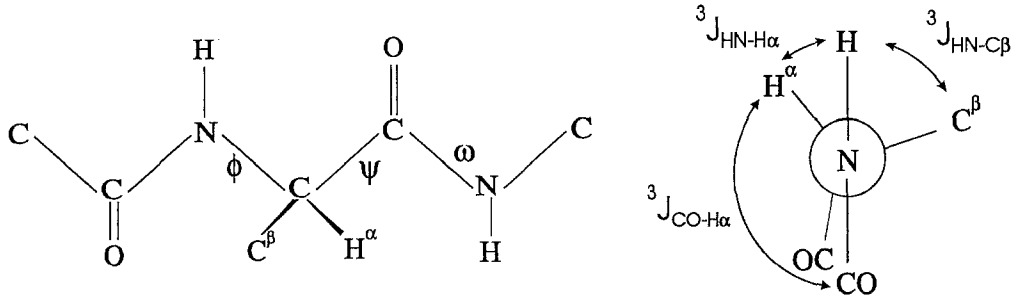

Fig. 2. Newman projection of the coupling constants containing information about the ϕ dihedral angle of a peptide backbone.

of these additional coupling constants produces up to four (sometimes two, depending on the coupling and the A, B and C parameters) allowed dihedral angles. A simple comparison of the allowed torsions for each coupling usually produces a rough agreement [22,23]. However, the coupling constants are still being used only as a secondary check, and not utilized in the development of the peptide conformation.

One method to utilize coupling constants in the computational refinement of the structure is the application of dihedral angle restraints, either to one particular value or to a range of allowed values [25–27]. The most common application of this method is the use of only 'extreme' coupling constants. As can be seen in Fig. 1, $^3J_{HN\text{-}H\alpha}$, couplings greater than 8.7 Hz produce only two values, centered about a ϕ of −120°. Therefore, for such couplings a dihedral angle restraint would be applied, restricting the torsion to −120° [25] or to a small range of values centered about this value [26,27]. Often 8.0 Hz is utilized as the cutoff for 'extreme' coupling constants and the possibility of a positive ϕ dihedral angle is ignored, which is based on the fact that in protein structures positive ϕ values are seldom observed. Similar approximations are commonly used for small coupling constants. However, in the examination of peptides, either cyclized or containing unusual amino acids, the possibility of positive ϕ dihedral angles cannot be excluded. In fact, there are many examples of such dihedral angles in peptides.

An approach that overcomes this problem was suggested by Kim and Prestegard [21]. The penalty function directly utilizes the measured coupling constant and the Karplus curve:

$$V_J = \tfrac{1}{2} K_J (J_{exp} - J_{theo})^2 \qquad (2)$$

where J_{exp} is the experimental coupling constant, K_J is a force constant to weigh each coupling individually and J_{theo} is the theoretical coupling calculated using Eq. 1. This function can be applied without any approximations of allowed dihedral angles, in contrast to dihedral angle restraining. The most important advantage of this formalism is the application of multiple coupling constants; each experimentally determined coupling constant can be included as an experimental restraint [28,29]. Each of the couplings can be individually scaled, according to the error of the experimental values and the confidence in the A, B and C coefficients of Eq. 1 (i.e., the homonuclear coupling constants as a general rule are determined with less error than the heteronuclear couplings). As an example of the usefulness of this method a profile of the penalty violation, 'energy', is given in Fig. 3. The inclusion of the heteronuclear coupling constants rules

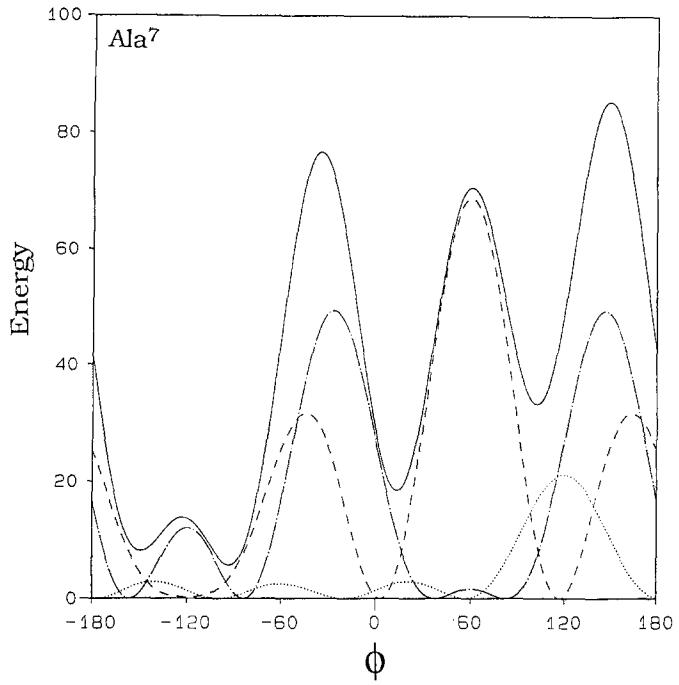

Fig. 3. Profile of the violation 'energy' for the ϕ torsions for three coupling constants measured for Ala^7 of cyclosporin A: $^3J_{HN\text{-}H\alpha}$ (dot-dash), $^3J_{HN\text{-}C\beta}$ (dot) and $^3J_{CO(i-1)\text{-}H\alpha}$ (dash), and for the sum of the functions (solid line).

out many of the values allowed by the homonuclear coupling. The use of this method has been illustrated for a number of cyclic peptides [28,29].

Although there are several different coupling constants that can be measured for ϕ and for the side-chain (e.g., χ^1, χ^2) dihedral angles, there are no three-bond coupling constants that can be easily obtained for the ψ torsion. The available couplings, i.e. $^3J_{N\text{-}H\alpha}$ (see Fig. 2), are very difficult to measure and are small, and therefore have a large experimental error. However, Egli and Von Philipsborn [30] have proposed a relationship for the heteronuclear one-bond coupling between the α-carbon and -proton, $^1J_{H\alpha\text{-}C\alpha}$, with dependence on both the ϕ and ψ torsions. This expression,

$$^1J = A + B\cos^2(\phi + 30°) + C\cos^2(\psi - 30°) \quad (3)$$

incorporated into a penalty function (Eq. 2), has produced very promising results; the three-bond couplings yield a small range of allowed torsions while the one-bond couplings supply information on the ψ dihedral angle [31]. An example 'energy' violation profile for a $^1J_{C\alpha\text{-}H\alpha}$ of 140 Hz is shown in Fig. 4. One advantage of the one-bond coupling is the ease of measurement, simply via a heteronuclear multiple-quantum correlation spectrum [32] without decoupling of the carbons during acquisition of the proton signal. Recently a new equation has been developed for the one-bond coupling constant [33]. The results using this relation are very similar to those obtained with Eq. 3.

One serious drawback of the application of coupling constant restraints in computational

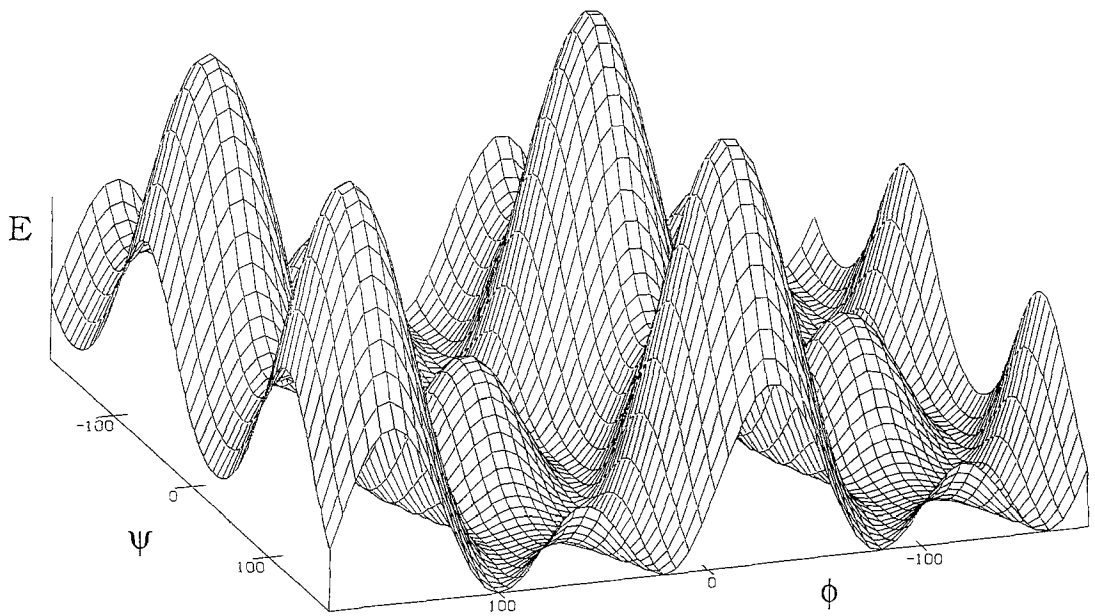

Fig. 4. The violation 'energy' for a one-bond $^{1}J_{C\alpha\text{-}H\alpha}$ coupling of 140 Hz, calculated using Eqs. 2 and 3.

refinement is the possibility of conformational mobility; the measured coupling is clearly an averaged quantity. The averaging can be thought of as an average of one structure over time which has led to the development of time-dependent experimental restraints, first applied with NOEs [34,35] and recently with coupling constants [36]. The energies and forces are calculated from the restraints averaged over a specific time span, allowing for flexibility on the time scale over which the restraints are averaged.

Another approach is to treat the coupling constants as an instantaneous average over an ensemble of structures. The utilization of multiple copies of the system and application of NOEs as 'effective restraints' (i.e., the energies and forces for the restraints are derived from the average of the ensemble) have been previously described [37]. The addition of coupling constants to this ensemble method has been utilized [38] to reproduce the correct population of side-chain rotamers, as predicted by the Pachler equation [39].

Although these two approaches for averaging of experimental restraints appear different and in practice will be carried out using different computational methods, theoretically both must produce the same result. Here, we compare the use of time-dependent restraints and the ensemble method with the application of both NOEs and coupling constant restraints. The methods are illustrated for extended calculations carried out on cyclosporin A (CsA), for which 117 NOEs and 62 homo- and heteronuclear coupling constants have been measured [29,40].

EXPERIMENTAL METHODS

Coupling constant restraints

The coupling constant restraints were applied in molecular dynamics simulations and in a

TABLE 1
EXPERIMENTAL AND CALCULATED COUPLING CONSTANTS FROM MD SIMULATIONS USING TIME-DEPENDENT NOE AND COUPLING CONSTANT RESTRAINTS AND AN ENSEMBLE CALCULATION OF CYCLOSPORIN A

Residue	Dihedral angle	Three-bond coupling[a]	Coupling constant (Hz)		
			Exp.	td-MD	Ensemble
MeBmt[1]	ϕ	$^3J_{H\alpha\text{-}C(i-1)}$	5.0	3.5	3.9
	χ^1	$^3J_{H\alpha\text{-}H\beta}$ (*S*)	6.0	6.1	5.9
		$^3J_{H\alpha\text{-}C\gamma}$	0.5	2.7	0.5
Abu[2]	ϕ	$^3J_{HN\text{-}H\alpha}$	9.9	9.2	9.9
	χ^1	$^3J_{H\alpha\text{-}H\beta}$ (*R*)	7.1	6.9	6.6
		$^3J_{H\alpha\text{-}H\beta}$ (*S*)	8.0	5.6	7.0
		$^3J_{C\text{-}H\beta}$ (*R*)	1.9	3.5	3.0
		$^3J_{C\text{-}H\beta}$ (*S*)	4.7	3.4	4.1
MeLeu[4]	ϕ	$^3J_{H\alpha\text{-}C(i-1)}$	2.5	3.2	2.5
	χ^1	$^3J_{H\alpha\text{-}H\beta}$ (*R*)	11.8	10.4	11.3
		$^3J_{H\alpha\text{-}H\beta}$ (*S*)	4.2	3.4	4.2
		$^3J_{C\text{-}H\beta}$ (*R*)	2.9	1.8	2.2
		$^3J_{C\text{-}H\beta}$ (*S*)	1.8	2.0	1.3
	χ^2	$^3J_{H\beta\text{-}C\delta}$ (*R*,*R*)	2.7	3.5	3.3
		$^3J_{H\beta\text{-}C\delta}$ (*S*,*R*)	2.2	3.5	4.0
		$^3J_{H\beta\text{-}C\delta}$ (*R*,*S*)	6.7	8.9	8.5
		$^3J_{H\beta\text{-}C\delta}$ (*S*,*S*)	2.2	3.5	3.3
Val[5]	ϕ	$^3J_{HN\text{-}H\alpha}$	8.5	9.0	8.5
		$^3J_{HN\text{-}C\beta}$	1.4	1.2	1.4
		$^3J_{H\alpha\text{-}C(i-1)}$	2.7	2.6	2.7
	χ^1	$^3J_{H\alpha\text{-}H\beta}$	9.8	11.4	10.7
		$^3J_{H\alpha\text{-}C\gamma}$ (*R*)	1.0	2.0	1.8
		$^3J_{H\alpha\text{-}C\gamma}$ (*S*)	3.2	3.1	4.0
MeLeu[6]	χ^1	$^3J_{H\alpha\text{-}H\beta}$ (*R*)	6.0	4.9	5.8
		$^3J_{H\alpha\text{-}H\beta}$ (*S*)	10.3	9.4	10.0
		$^3J_{C\text{-}H\beta}$ (*R*)	7.3	7.4	7.6
		$^3J_{C\text{-}H\beta}$ (*S*)	1.5	1.8	1.3
	χ^2	$^3J_{H\beta\text{-}C\delta}$ (*R*,*R*)	3.0	4.5	4.0
		$^3J_{H\beta\text{-}C\delta}$ (*S*,*R*)	6.0	7.7	7.6
		$^3J_{H\beta\text{-}C\delta}$ (*R*,*S*)	2.6	3.7	4.3
		$^3J_{H\beta\text{-}C\delta}$ (*S*,*S*)	3.4	4.5	4.0
Ala[7]	ϕ	$^3J_{HN\text{-}H\alpha}$	7.4	9.6	7.4
		$^3J_{HN\text{-}C\beta}$	1.4	1.3	1.5
		$^3J_{H\alpha\text{-}C(i-1)}$	4.3	2.9	4.3
D-Ala[8]	ϕ	$^3J_{HN\text{-}H\alpha}$	8.0	8.5	8.0
		$^3J_{HN\text{-}C\beta}$	1.0	1.6	1.0
		$^3J_{H\alpha\text{-}C(i-1)}$	2.4	2.3	2.4
MeLeu[9]	ϕ	$^3J_{H\alpha\text{-}C(i-1)}$	2.7	3.3	2.7
	χ^1	$^3J_{H\alpha\text{-}H\beta}$ (*R*)	11.2	9.4	9.6
		$^3J_{H\alpha\text{-}H\beta}$ (*S*)	4.6	4.4	4.6
	χ^2	$^3J_{H\beta\text{-}C\delta}$ (*R*,*R*)	4.4	4.8	3.6
		$^3J_{H\beta\text{-}C\delta}$ (*S*,*R*)	2.0	3.7	3.5
		$^3J_{H\beta\text{-}C\delta}$ (*R*,*S*)	5.3	7.4	3.6
		$^3J_{H\beta\text{-}C\delta}$ (*S*,*S*)	2.6	4.8	3.5
MeLeu[10]	χ^1	$^3J_{H\alpha\text{-}H\beta}$ (*R*)	8.2	7.0	8.2
		$^3J_{H\alpha\text{-}H\beta}$ (*S*)	6.5	6.1	6.4

TABLE 1 (continued)

Residue	Dihedral angle	Three-bond coupling[a]	Coupling constant (Hz)		
			Exp.	td-MD	Ensemble
MeLeu[10]	χ^2	$^3J_{H\beta\text{-}C\delta}$ (*R,R*)	3.8	3.9	3.8
		$^3J_{H\beta\text{-}C\delta}$ (*S,R*)	4.5	5.0	4.5
MeVal[11]	ϕ	$^3J_{H\alpha\text{-}C(i-1)}$	3.4	3.5	3.4
	χ^1	$^3J_{H\alpha\text{-}H\beta}$	11.0	10.8	11.6
		$^3J_{H\alpha\text{-}C\gamma}$ (*R*)	1.2	2.0	1.8
		$^3J_{H\alpha\text{-}C\gamma}$ (*S*)	2.5	3.7	3.1

[a] The β protons and the γ and δ methyl groups of the side chains of the valines and leucines have been diastereotopically assigned [40]; assignments are indicated in parentheses.

modified distance-bounds-driven dynamics refinement protocol using Eq. 2, following procedures previously described [21,28,38]. The molecular motions which affect the coupling constants are accounted for by modification of the calculation of the theoretical coupling constant used in Eq. 2. The time-dependent method calculates the time average of the $\cos(\theta)$ series:

$$\langle \cos^m \theta(t) \rangle = [1 - \exp(-\Delta t/\tau)] \cos^m \theta(t) + \exp(-\Delta t/\tau) \langle \cos^m (t-\tau) \rangle \quad (4)$$

where Δt is the time step of the simulation. The exponential time decay is used so that the average restraint is still effective, even with long simulation trajectories. Equation 4 is then used to calculate J_{theo}:

$$J_{theo} = A \langle \cos^2 \theta \rangle + B \langle \cos \theta \rangle + C \quad (5)$$

which is used in Eq. 2 to calculate the penalty function [36].

Within the ensemble method multiple copies of the molecule are utilized, and J_{theo} is calculated by a simple average of the couplings for each member of the ensemble:

$$\langle J_{theo} \rangle = \frac{1}{N} \sum_{i=1}^{N} J_i \quad (6)$$

This average value is used to calculate the energies and forces following Eq. 2, which are then applied to each member of the ensemble. Each member of the ensemble may be well away from the 'target' coupling constant, but if the average as calculated from Eq. 6 is in agreement with the experimental value, the penalty function (Eq. 2) is zero and no forces are applied.

For both of the calculations, the 117 NOEs previously reported were utilized as restraints [40]. For the upper and lower distance restraints, respectively, 5% was added to or subtracted from the NOE-derived distance. In addition, the 62 coupling constants as previously described [29] (listed in Table 1), were also utilized as restraints.

Time-dependent restraints

The MD simulations with time-dependent NOE and coupling constant restraints were carried out in vacuo with the stochastic dynamics (SD) module within GROMOS [41], solving the

Langevin equation of motion [42]. In SD calculations, the solvent is treated as a virtual surrounding, calculated by a stochastic force and a force proportional to the velocity and relative friction coefficient, which mimic collisions of the solute with the solvent. The relative friction coefficient is evaluated by Stoke's law of friction and is scaled by a relative solvent-accessible area factor [36]. The parameters used to mimic the solvent were derived from CCl_4.

The step size for the simulation was set to 2 fs using SHAKE [43], with the nonbonded interactions updated every 50 steps. A cutoff radius of 10 nm and a tight coupling to a temperature bath [44] (100 fs relaxation time) were used. The force constant for the coupling constants was 2.0 kJ mol^{-1} Hz^{-2} with a relaxation delay time, τ, (Eq. 4) of 20 ps.

Ensemble calculations

The ensemble-averaged restraints were applied using a modified version of the simplified dynamics program, distance-bound-driven dynamics (DDD) [45], which includes the option for coupling constant restraints (called DADD for distance- and angle-driven dynamics) [38]. For our calculations, 50 structures were produced by the random metrization procedure [46,47], which were then refined with DDD using constant NOE and coupling constant restraints. The 'force field' of the DDD calculations is

$$V = V_{Hol} + V_{NOE} + V_j \tag{7}$$

The holonomic expression, V_{Hol}, maintains the topology of the molecule using oriented chiral volumes and a matrix of upper and lower bounds on the interatomic distances [37,46,48]. The V_{NOE} and V_j are standard penalty terms, similar to that shown in Eq. 2. The ensemble calculations are identical to those used for the DDD method, but with the forces from the experimental observations calculated from an ensemble average of all the structures [37,38]. To create a starting ensemble of structures, the 21 lowest energy structures from the DDD calculations discussed above were copied 20 times each, creating an ensemble of 420 molecules. The ensemble calculations were carried out for 10 000 steps with a step size of 20 fs at a temperature of 500 K and with a tight coupling to a temperature bath [44]. After this the temperature was slowly decreased during 2500 steps by weak coupling to a temperature bath of 1 K.

RESULTS AND DISCUSSION

The coupling constants calculated from the time-dependent MD simulations and the ensemble calculations are given, along with the experimental values, in Table 1. The coupling constants were calculated for each structure of the trajectory or ensemble and then averaged. The coupling constant from the average dihedral angle will produce quite different, and for our purposes false, answers. The average dihedral angles from the two calculations are given in Table 2. The standard deviation of the angles were calculated from the trajectory of the time-dependent MD simulation, using standard methods [41]. To obtain a measure of the range of values from the ensemble method, the dihedral angle deviation (dhad) [46] was calculated.

The experimental coupling constants from both methods are mostly well reproduced. The couplings involving backbone dihedral angles are in especially good agreement, one exception being the values for Ala^7 from the time-dependent calculation. The results from the ensemble

calculation are much better, but the range of values observed for torsion angle ϕ of Ala[7] is extremely large (i.e., a dhad of 80°). However, for the present discussion the coupling constants of the side chains are of greater interest, since dynamics and molecular motions certainly play an important role.

TABLE 2
AVERAGE DIHEDRAL ANGLES FROM MD SIMULATION USING TIME-DEPENDENT RESTRAINTS AND AN ENSEMBLE CALCULATION OF CYCLOSPORIN A

			td-MD		Ensemble	
Residue	Dihedral angle	MD ave.	Ave.	S.D.[a]	Ave.	Dhad[b]
MeBmt[1]	ϕ	−89	−110	9	−119	17
	ψ	112	112	24	120	13
	χ^1	−77	176	>100	−41	12
Abu[2]	ϕ	−97	−103	20	−103	19
	ψ	100	94	14	54	45
	χ^1	−70	−72	67	1	54
Sar[3]	ϕ	79	68	17	101	43
	ψ	−108	−120	20	−123	53
MeLeu[4]	ϕ	−122	−107	13	−96	18
	ψ	30	32	23	−3	22
	χ^1	−151	−80	29	−79	68
	χ^2	−172	−96	54	−38	54
Val[5]	ϕ	−104	−103	22	−132	60
	ψ	123	120	11	149	30
	χ^1	−61	−56	30	−66	35
MeLeu[6]	ϕ	−82	−93	13	−117	28
	ψ	88	106	23	97	33
	χ^1	−178	−155	29	−46	88
	χ^2	−175	−134	54	38	63
Ala[7]	ϕ	−67	−102	12	−50	80
	ψ	54	58	23	23	46
D-Ala[8]	ϕ	80	96	19	67	48
	ψ	−137	−128	12	−132	19
MeLeu[9]	ϕ	−125	−132	11	−136	27
	ψ	116	110	12	110	23
	χ^1	−60	−110	65	−45	30
	χ^2	−70	−103	42	−161	52
MeLeu[10]	ϕ	−131	−119	10	−128	32
	ψ	86	99	14	95	25
	χ^1	−148	−119	45	−82	68
	χ^2	−78	−106	40	−164	61
MeVal[11]	ϕ	−120	−115	12	−112	16
	ψ	133	118	16	162	8
	χ^1	−60	−151	>100	−66	18

The results from a previous MD simulation [40] using only NOE restraints are given for comparison.

[a] The standard deviation has been calculated from the trajectory of Cartesian coordinates, following the standard procedure of finding the minimum rotation between the current and previous value [41].

[b] For the ensemble calculation, the deviation of the dihedral angle, dhad, has been calculated, following published procedures [46].

The results of the side-chain couplings are also good. For the χ^1 torsion, the couplings are in good agreement with the experimental values. The exception is the χ^1 value of the MeBmt from the MD simulations. The problem can be associated with the hydroxyl group of this amino acid, i.e., the partial charges of this group stabilize a hydrogen bond with the carbonyl of the backbone. This is an artifact of the in vacuo calculation. Similar artifacts have been documented in the literature [49–51]. The simplest answer is the use of explicit solvent, which for chloroform has recently been demonstrated [52–54]. However, the time required for such simulations increases dramatically and the question of obtaining enough time periods (τ) over which the restraints are averaged to obtain good statistics is a concern [36]. Here, the MD simulations have been carried out using the SD method in an attempt to mimic the solvent; the greater the solvent exposure of an atom, the greater the friction to mimic collisions with the solvent. However, in vacuo effects are still persistent, indicating that perhaps a more complex description of the solvent is required [55]. The average χ^1 dihedral angle from the ensemble method displays some deviation from the values previously obtained [40], see Table 2. Part of this problem is caused by the averaging of the torsions. A better representation of the results is given in Fig. 5. Here, the values for the complete ensemble are shown for these side-chain torsions. It is important to note that for the most part the three staggered rotamers are observed, even though within the ensemble method there is no dihedral angle expression to forbid the eclipsed rotamers. The combination of the coupling constants and the NOEs naturally creates the preference for the staggered rotamers. The side chain of Abu[2] is an exception, showing a smeared distribution from −60 to 60°, which explains the average dihedral angle of 1° (Table 2).

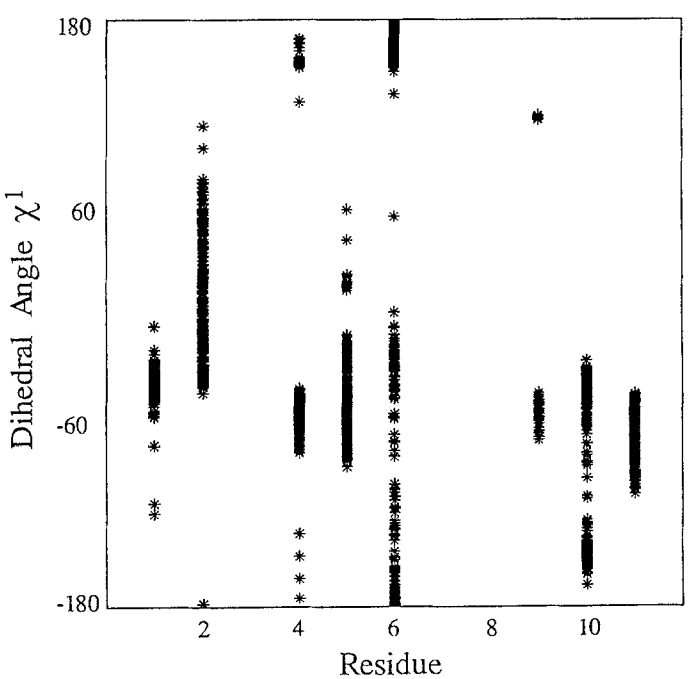

Fig. 5. A plot of the χ^1 dihedral angles for the residues of cyclosporin A obtained from an ensemble calculation of 420 structures.

There is a much larger deviation of the experimental and theoretical coupling constants with the χ^2 dihedral angle. This is true with both calculation procedures. The reasons for the deviations could arise from the obviously greater flexibility of these torsions, much greater than observed for the χ^1 torsions. One consequence of this flexibility is that there are far fewer NOEs to help in the definition of these dihedral angles. Another important point concerning the χ^2 torsion is the A, B and C coefficients used in Eq. 1. These coefficients have not been developed specifically for these coupling constants, but were calculated from more general $^3J_{H\text{-}C}$ couplings [11].

Both of the computational approaches reproduce the structure calculated previously using only NOE restraints [40], see Table 2. There are some small differences, particularly with the side-chain torsions as discussed above. Some problems mentioned above with the time-dependent restraints must be attributed, not to the application of the restraints, but to the MD method in general (i.e., the necessity to use solvent to avoid in vacuo effects). On the other hand, the 'force field' utilized in the ensemble calculations is too simple for most practical purposes. If 'realistic' energies are required for comparative purposes, the structures will need to be further examined with a full molecular mechanics force field. As far as computational requirements are concerned, the methods are similar in CPU usage. This, of course, will change drastically if explicit solvents are required. The ensemble method, utilizing a distance bounds matrix created from standard DG methods, requires much more memory than the MD method.

CONCLUSIONS

In this article the use of coupling constants as experimental restraints in computer structural refinement has been reviewed. To account for the obvious averaging of the coupling constants, two different approaches have been compared. Cyclosporin A was examined since the structure in chloroform is extremely well determined [40] and there are a large number of both coupling constants and NOEs. Both methods reproduce the coupling constants quite well.

ACKNOWLEDGEMENTS

The contributions to this article from Matthias Eberstadt, Simona Golic Grdadolnik, Dr. Matthias Köck, and Dr. Peter Schmieder are gratefully acknowledged. We thank Dr. Ruud Scheek (University of Groningen) for the distance geometry and associated programs. The Deutsche Forschungsgemeinschaft and the Fonds der Chemischen Industrie are gratefully acknowledged for financial support.

REFERENCES

1 Kessler, H., Angew. Chem., Int. Ed. Engl., 21 (1982) 512.
2 Schiller, P.W., In Udenfriend, S. and Meienhofer, J. (Eds.) The Peptides, Vol. 6, Academic Press, Orlando, FL, 1984, pp. 219–268.
3 Hruby, V.J., Al-Obeidi, F. and Kazmierski, W., Biochem. J., 268 (1990) 249.
4 Veber, D.H., Holly, F.W., Paleveda, W.J., Nutt, R.F., Bergstrand, S.J., Torchiana, M., Glitzer, M.S., Saperstein, R. and Hirschmann, R., Proc. Natl. Acad. Sci. USA, 75 (1978) 2636.
5 Kessler, H. and Kutscher, B., Tetrahedron Lett., 26 (1985) 177.
6 Lautz, J., Kessler, H., Boelens, R., Kaptein, R. and Van Gunsteren, W.F., Int. J. Pept. Protein Res., 30 (1987) 404.
7 Aumailley, M., Gurrath, M., Müller, G., Calvete, J., Timpl, R. and Kessler, H., FEBS Lett., 291 (1991) 50.

8 Saulitis, J., Mierke, D.F., Byk, G., Gilon, C. and Kessler, H., J. Am. Chem. Soc., 114 (1992) 4814.
9 Hruby, V.J., Biopolymers, 33 (1993) 1073.
10 Karplus, M., J. Am. Chem. Soc., 85 (1963) 2870.
11 Bystrov, V.F., Prog. NMR Spectrosc., 10 (1976) 41.
12 Schmieder, P. and Kessler, H., Biopolymers, 32 (1992) 435.
13 Kessler, H., Griesinger, C., Zarbock, J. and Loosli, H.R., J. Magn. Reson., 57 (1984) 331.
14 Kessler, H., Bermel, W. and Griesinger, C., J. Am. Chem. Soc., 107 (1986) 1083.
15 Montelione, G.T., Winkler, M.E., Rauenbuehler, P. and Wagner, G., J. Magn. Reson., 82 (1989) 198.
16 Neri, D., Otting, G. and Wüthrich, K., J. Am. Chem. Soc., 112 (1990) 3663.
17 Kay, L.E. and Bax, A., J. Magn. Reson., 86 (1990) 110.
18 Montelione, G.T. and Wagner, G., J. Am. Chem. Soc., 111 (1989) 5474.
19 Keeler, J., Neuhaus, D. and Titman, J.J., J. Chem. Phys., 146 (1988) 545.
20 Titman, J.J., Neuhaus, D. and Keeler, J., J. Magn. Reson., 85 (1989) 111.
21 Kim, Y. and Prestegard, J.H., Protein Struct. Funct. Genet., 8 (1990) 377.
22 Schmieder, P., Kurz, M. and Kessler, H., J. Biomol. NMR, 1 (1991) 403.
23 Kurz, M., Schmieder, P. and Kessler, H., Angew. Chem., Int. Ed. Engl., 30 (1991) 1329.
24 Seip, S., Balbach, J. and Kessler, H., Angew. Chem., Int. Ed. Engl., 31 (1992) 1609.
25 De Vlieg, D., Boelens, R., Scheek, R.M., Kaptein, R. and Van Gunsteren, W.F., Isr. J. Chem., 27 (1986) 181.
26 Kline, A.D., Braun, W. and Wüthrich, K., J. Mol. Biol., 204 (1988) 675.
27 Moore, J.M., Case, D.A., Chazin, W.J., Gippert, G.P., Havel, T.F., Powls, R. and Wright, P.E., Science, 240 (1988) 314.
28 Mierke, D.F. and Kessler, H., Biopolymers, 32 (1992) 1277.
29 Eberstadt, M., Mierke, D.F., Köck, M. and Kessler, H., Helv. Chim. Acta, 75 (1992) 2583.
30 Egli, H. and Von Philipsborn, W., Helv. Chim. Acta, 64 (1981) 976.
31 Mierke, D.F., Golic Grdadolnik, S. and Kessler, H., J. Am. Chem. Soc., 114 (1992) 8283.
32 Bax, A. and Subramanian, S., J. Magn. Reson., 67 (1986) 565.
33 Vuister, G.W., Delaglio, F. and Bax, A., J. Am. Chem. Soc., 114 (1992) 9674.
34 Torda, A.E., Scheek, R.M. and Van Gunsteren, W.F., Chem. Phys. Lett., 157 (1989) 289.
35 Torda, A.E., Scheek, R.M. and Van Gunsteren, W.F., J. Mol. Biol., 214 (1990) 223.
36 Torda, A.E., Brunne, R.M., Huber, T., Kessler, H. and Van Gunsteren, W.F., J. Biomol. NMR, 3 (1993) 55.
37 Kemmink, J., Van Mierlo, C.P.M., Scheek, R.M. and Creighton, T.E., J. Mol. Biol., 230 (1993) 312.
38 Mierke, D.F., Scheek, R.M. and Kessler, H., Biopolymers, (1994) in press.
39 Pachler, K.G.R., Spectrochim. Acta, 19 (1963) 2085.
40 Kessler, H., Köck, M., Wein, T. and Gehrke, M., Helv. Chim. Acta, 73 (1990) 1818.
41 Van Gunsteren, W.F. and Berendsen, H.J.C., Groningen Molecular Simulation Library Manual (GROMOS), Biomos B.V., Groningen, 1987.
42 Van Gunsteren, W.F. and Berendsen, H.J.C., Mol. Simul., 1 (1988) 173.
43 Ryckaert, J.P., Ciccotti, G. and Berendsen, H.J.C., J. Comput. Phys., 23 (1977) 327.
44 Berendsen, H.J.C., Postma, J.P.M., Van Gunsteren, W.F., DiNola, A. and Haak, J.R., J. Chem. Phys., 81 (1984) 3684.
45 Kaptein, R., Boelens, R., Scheek, R.M. and Van Gunsteren, W.F., Biochemistry, 27 (1988) 5389.
46 Havel, T.F., Biopolymers, 29 (1990) 1565.
47 Havel, T.F., Prog. Biophys. Mol. Biol., 56 (1991) 43.
48 Crippen, G.M. and Havel, T.F., Distance Geometry and Molecular Conformation, Research Studies Press Ltd. (Wiley), New York, NY, 1988.
49 Mierke, D.F. and Kessler, H., J. Am. Chem. Soc., 113 (1991) 9466.
50 Levitt, M. and Saron, R., Proc. Natl. Acad. Sci. USA, 85 (1988) 7557.
51 Kurz, M., Mierke, D.F. and Kessler, H., Angew. Chem., Int. Ed. Engl., 31 (1992) 210.
52 Jorgensen, W.L. and Severance, D.L., J. Am. Chem. Soc., 112 (1990) 4768.
53 Konat, R.K., Mierke, D.F., Kessler, H., Kutscher, B., Bernd, M. and Voegeli, R., Helv. Chim. Acta, 76 (1993) 1649.
54 Brüschweiler, R., Roux, B., Blackledge, M., Griesinger, C., Karplus, M. and Ernst, R.R., J. Am. Chem. Soc., 114 (1992) 2289.
55 Gilson, M.K. and Honig, B., Protein Struct. Funct. Genet., 4 (1987) 7.